Proceedings of the XV$^{th}$ Bi-Annual Symposium on Measuring Techniques in Transonic and Supersonic Flows in Cascades and Turbomachines, 21-22 September, Florence, Italy

# The Aerodynamic Design and Use of Multi-Sensor Pressure Probes for MEMS Applications

**H. Babinsky, U. Kuschel, H. P. Hodson, D. F. Moore and M. E. Welland**
Cambridge University, Department of Engineering, Trumpington Street
Cambridge, CB2 1PZ, UK

## ABSTRACT

A family of novel planar geometries suitable for the construction of a MEMS (Micro-Electro-Mechanical-System)-based 5-hole flow sensor is introduced. The desired directional sensitivity is achieved by placing fences on the planar frontal surface of a cylindrical probe. The flow over such probes with and without fences has been investigated in a low speed wind tunnel at Reynolds numbers between 15,000 and 40,000 based on probe diameter. The potential of each design for use as a 5-sensor probe has been determined from pressure measurements and flow visualisations. It was found that fences could significantly increase the directional sensitivity of cylindrical probes. The best design tested had at least equivalent angular sensitivity compared to traditional 5-hole probes, while displaying no significant Reynolds number effects in the range tested.

## NOMENCLATURE

| | |
|---|---|
| $C_p$ | surface pressure coefficient, $(p - p_\infty)/0.5\rho U_\infty^2$ |
| D | probe head diameter |
| h | fence height |
| $K_1$, $K_2$ | directional calibration coefficients |
| $K_{dyn}$ | dynamic pressure calibration coefficient |
| $K_{pt}$ | total pressure calibration coefficient |
| p | pressure |
| q | dynamic pressure, $0.5\rho U_\infty^2$ |
| U | velocity |
| θ | pitch angle |
| ρ | density |
| ϕ | roll angle |

*Subscript*

| | |
|---|---|
| 0 – IV | sensor number |
| t | reservoir condition |
| • | freestream condition |

## INTRODUCTION

Many of the most challenging problems of aerodynamics today are concerned with highly unsteady and three-dimensional flows. Examples can be found throughout turbomachinery, in transonic flows, and also in the research into turbulent structures. Therefore, there is a great need for a sensor that is capable of determining velocity vectors with high spatial and temporal resolution. While non-intrusive optical techniques, such as Laser Doppler Anemometry (LDA) or Particle Image Velocimetry (PIV) are capable of providing such data, they are generally expensive, difficult to apply in certain situations, and require optical access to the region of interest. Hot-wires are relatively well established and can provide velocity information at very high frequencies, however, their size is still relatively large, they can be fragile and they may require significant effort in calibration.

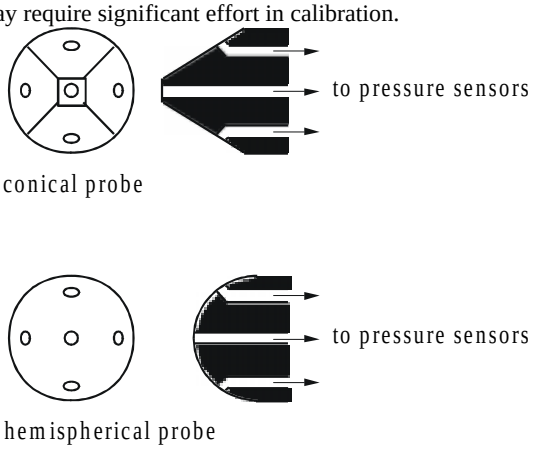


**Fig. 1 Traditional 5-hole probe designs**

Five-hole probes (see Fig. 1) are widely used[1] as a simple, robust and useful tool for the determination of velocity vectors, but there is usually a trade-off between their size and their frequency resolution. Several researchers[2,3,4] have attempted to build very small 5-hole probes, of the order of 1-2 mm in diameter, but in these cases the small size prevents the actual pressure transducers from being very close to the probe head and the frequency response is relatively poor. A different approach is to incorporate small

pressure transducers in the design of the probe itself in order to shorten any tubing between the pressure tapping and the sensor. This can give very good frequency response, however, the size of such a probe is relatively large, making it unsuitable for many flow applications.

Through the emergence of MEMS (Micro-Electro-Mechanical-Systems) technology[5,6] and its introduction into aeronautical sensor technology[7] there are now good prospects to fabricate a 5-hole probe which is both small in size and has the pressure sensors incorporated in the probe head itself. Such a solution promises to be extremely small in size (< 1 mm) and have a very high frequency response (> 100 kHz). However, there are still very significant problems with this approach, in particular due to the fact that MEMS technology has been developed from microelectronic fabrication processes, which are essentially planar systems. The construction of a complex 3-dimensional array of pressure sensors that would be needed for a micro-5-hole probe is not yet practical. Redionitis and co-workers[8,9] have suggested ways to bypass this difficulty by manufacturing an array of 5 miniature pressure sensors located in a plane. They mount a hemisphere fitted with pressure tappings (with a similar geometry to Fig. 1b) on the surface above this array, and connect the pressure holes to the respective pressure sensor underneath, thus keeping the amount of tubing between the pressure tapping position and the pressure sensor to a minimum. They have shown that, in principle, such an approach is feasible and could lead to a 5-hole probe of approximately 1 mm diameter with a high frequency response. The difficulties with this approach are that the hemisphere containing the tubes needs to be manufactured and assembled with the sensor array. This therefore limits the minimum size that can be achieved. Furthermore, the length and the small diameter of the connections between the pressure sensors and the relevant pressure tapping on the hemisphere surface have a deleterious effect on the response time.

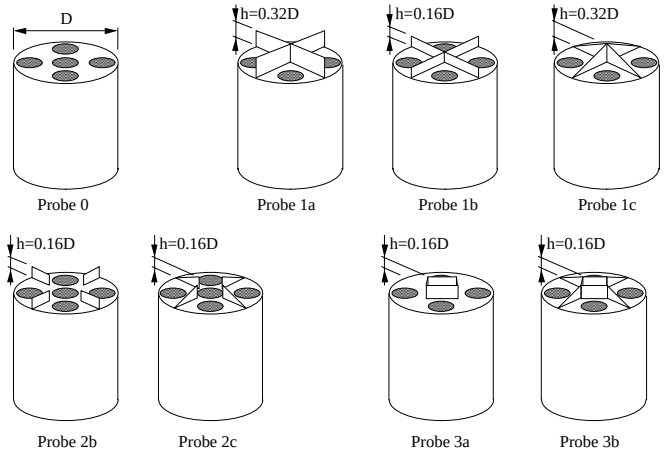


**Fig. 2 Probe designs tested**

The novel approach suggested in this paper is to propose miniature 5-sensor probes with a head geometry that can be manufactured entirely using MEMS technology without post assembly. As seen in Fig. 2, the sensing elements are arranged in a plane in a fashion similar to that described by Redionitis and Vijayagopal[9]. However, here these sensors are exposed directly to the flow and the desired sensitivity of the probe is achieved by fitting flow manipulating fences protruding above the sensor plane. Such fences can be constructed using MEMS technology provided that the typical dimensions are relatively small compared to the probe head diameter and that the geometry of flow manipulating devices is kept simple. For example, one promising route to construct flow manipulating devices and miniature fences of the types shown in Fig. 2 is to make the protruding structures out of hardened photoresist[5].

It is the aim of this paper to investigate to what extent planar configurations such as those sketched in Fig. 2 are suitable for the design of a miniature 5-sensor probe, and how their sensitivity and range of application compare with a traditional 5-hole probe design. First, the flow over a simple planar cylindrical probe (Probe 0 in Fig. 2) is investigated and then various fences are added with the aim of manipulating the flow and modifying the surface pressure distributions. The effect of simple fences is investigated with probes 1a-c, while more complex geometries suitable for 5-sensor probes are studied with models 2b, 2c, 3a and 3b. In all cases the local flowfield is examined in detail in order to provide pointers for the critical features of a potential probe design.

## EXPERIMENTAL METHOD

Large scale models were tested in one of the Department's low-speed wind tunnels featuring a square working section (0.7 m × 0.5 m) and capable of speeds between 6 m/s and 25 m/s. All probes were based on a generic probe head (shown in Fig. 3) fitted with 41 pressure holes of 0.25 mm diameter and grooves to hold any of the fence configurations seen in Fig. 2. Fences were constructed from metal sheets of 0.25 mm thickness. The Reynolds number based on probe diameter varied between 15,000 and 40,000. The probe head was mounted on a cylindrical sting that could be adjusted for roll and angle of attack. Fig. 4 shows a probe mounted in the working section of the wind tunnel and Fig. 5 shows a schematic drawing of the co-ordinate system used in the investigation. Typical measurements for each probe investigated the range of 0°-45° in pitch angle $\theta$ (in steps of 5°) and 0° - 45° in roll angle $\phi$ (in steps of 11.25°). The pressure distribution at all other roll angles was inferred by assuming symmetrical behaviour.

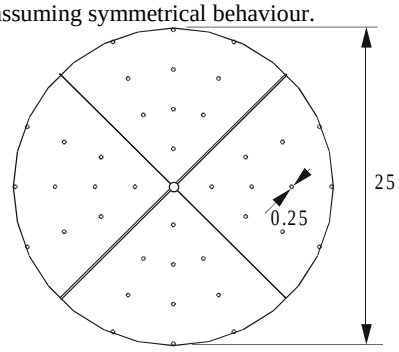


**Fig. 3 Probe head showing the 41 pressure tapping positions**

The free stream flow conditions were determined with a Pitot-static tube connected to an electronic manometer and mounted in the working section of the wind tunnel.

In order to gain further understanding of the flow physics around fenced probes several 'dummy' models without pressure tappings were also manufactured to be used for flow visualisation studies. In particular, oil-flow visualisation was used in the low speed wind tunnel and a smaller specialised tunnel was used for smoke flow visualisations. While oil-flow visualisation was performed at the same Reynolds numbers as the quantitative experiments, the Reynolds number of the smoke flow experiments

was only of the order of 3000. Nevertheless, these experiments provided valuable insight into the flow patterns over the probe geometries.

**Fig. 4 Probe mounted in a low-speed wind tunnel**

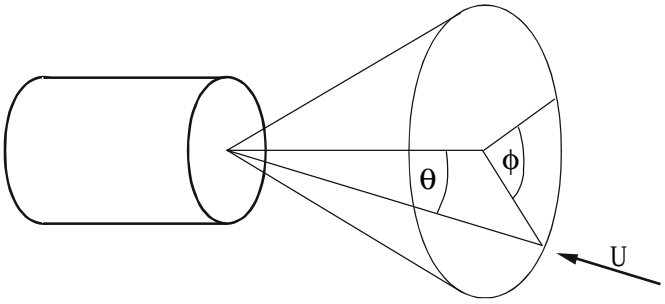


**Fig. 5 Pitch (θ) and roll (ϕ) co-ordinate system**

## Errors

All surface pressures were read from an inclined U-tube manometer filled with alcohol. The wind tunnel speed was set using a digital manometer connected to a Pitot-static probe. Taking errors of both devices into account, the total inaccuracy in determining a pressure coefficient was ±13% for Re = 15,000 and ±2% for Re = 40,000. All of the results shown here have been obtained at Re = 40,000. It was also found that the probe mount exhibited a degree of flexibility which introduced an error ± 2° in roll angle and ± 3° in pitch angle.

## RESULTS

### Planar probe without fences

Fig. 6 shows surface pressure distributions as well as results of the oil-flow visualisation on the planar probe for several pitch angles. It can be seen that the flowfield is relatively straightforward; with increasing angle of attack the stagnation point moves towards the edge of the probe surface. It is interesting to note that the pressure distribution along the frontal surface varies with angle of attack and therefore even the flat end of a cylinder has some potential for a 5-sensor probe.

### Effect of fences mounted on the probe surface

The introduction of fences dramatically changes the flow over the probe head. It was found that for non-zero angles of attack a separation bubble formed on the leeward side of each fence. This is seen clearly by the smoke-flow visualisation for probe 1a as shown in Fig. 7. Fig. 7a shows the flow for zero pitch angle while Fig. 7b to Fig. 7e show the flowfield for pitch angles in the range 0° - 50°. Closer investigation revealed the presence of secondary separation bubbles at the base of each fence. The appearance of separation leads to the formation of a low pressure region in the leeward side of each fence, and it was found that the pressure in this region decreases with increasing angle of attack and separation bubble size. This is demonstrated by the pressure distributions (a selection is given in Fig. 8) when compared to the smoke flow visualisations of Fig. 7 and the equivalent results for the strictly planar probe (Fig. 6).

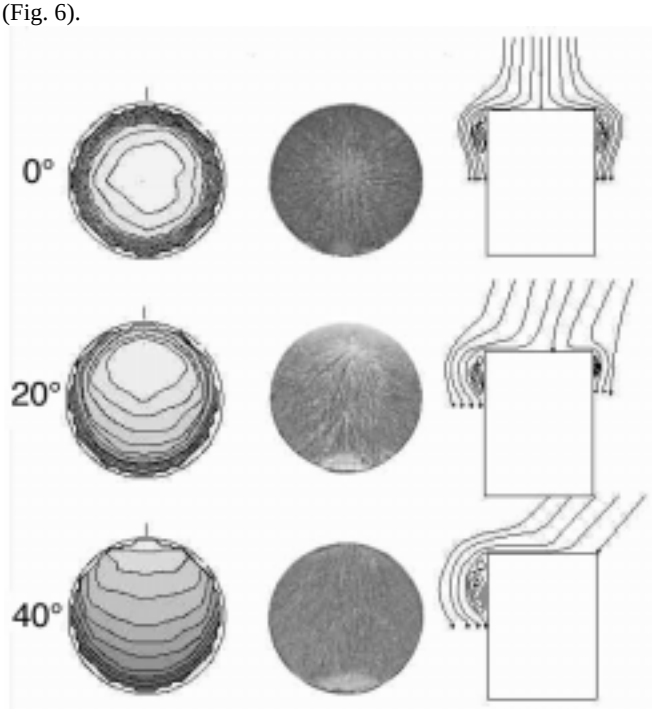


**Fig. 6 Surface pressure distribution and oil-flow visualisation for a cylindrical probe at various pitch angles**

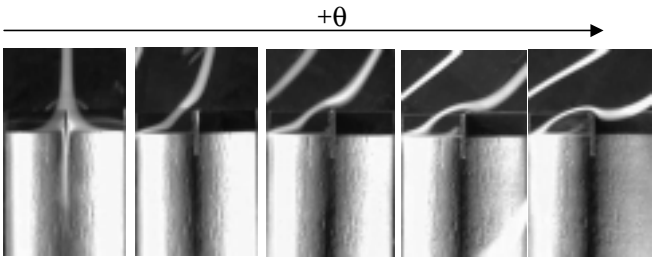


**Fig. 7 Flow over Probe 1a at increasing pitch angle, Fig. (a) is at zero pitch. A separation bubble forms on the leeward side of the fence. The bubble size increases with pitch angle.**

The effect of fence height is demonstrated when the results obtained for probes 1a and 1b are compared. Probe 1a featured a fence height of $0.32 \times D$, whereas probe 1b featured a fence height of $0.16 \times D$. A selection of typical pressure distributions for model 1b is given in Fig. 9. It can be seen that the change in fence height does not lead to a fundamentally different flowfield, however the pressure differences between leeward and windward sides are more pronounced for taller fences. While a larger fence height appears to be more sensitive, i.e. offers a larger pressure variation for a given

change in angle of attack, it is expected that the smaller fence will offer more uniform sensitivity up to higher pitch angles.

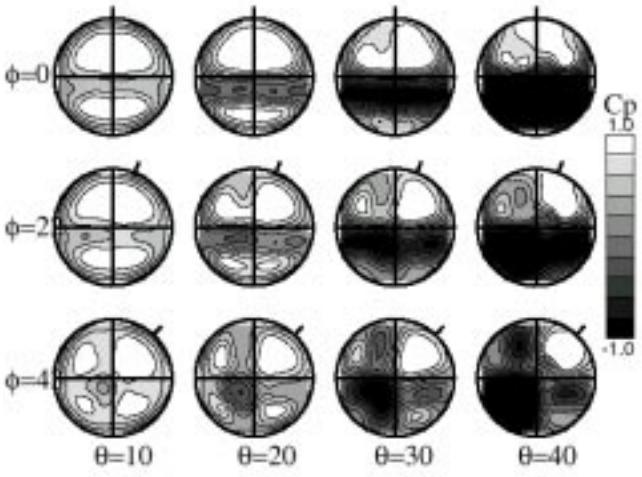


**Fig. 8 Selection of measured surface pressure distributions on Probe 1a (h/D=0.32) for various pitch and roll angles (the flag near the top of each plot indicates the relative flow direction).**

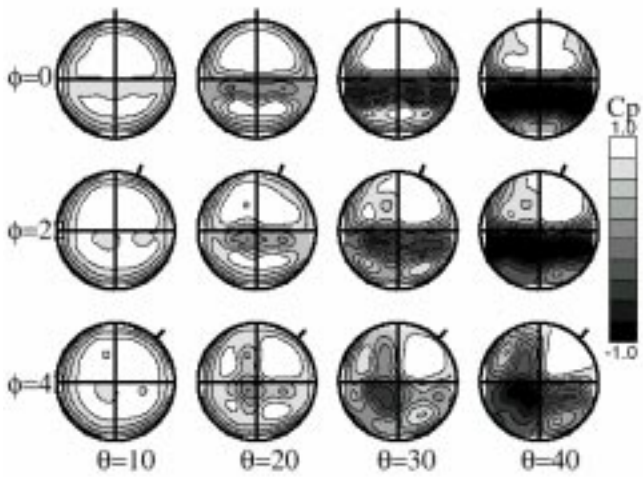


**Fig. 9 Selection of measured surface pressure distributions on Probe 1b (h/D=0.16) for various pitch and roll angles (the flag near the top of each plot indicates the relative flow direction).**

The effect of fence shape was investigated with probe 1c where 'delta-type' fences were fitted with a maximum height of $0.32 \times D$ at the centre. Typical pressure distributions are given in Fig. 10. It can be seen that the pressure distributions are comparable to those obtained with probe 1b. There is no fundamental difference in the flow patterns between this probe and straight fence designs.

## Fenced probes suitable for 5-sensor arrays

All geometries investigated so far have proven to be very sensitive to flow angle variations throughout the tested range. However, due to the fence geometry it would not be possible to mount a central hole, and neither geometry would be suitable for the design of a 5-sensor probe. Therefore, a range of designs with space for a central sensor was tested.

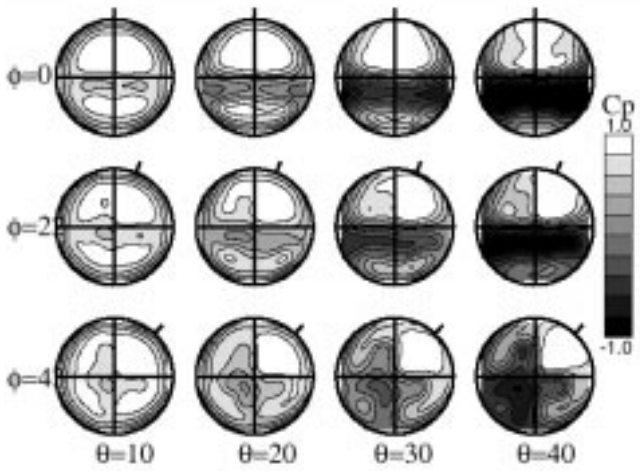


**Fig. 10 Selection of measured surface pressure distributions on Probe 1c (delta fences) for various pitch and roll angles (the flag near the top of each plot indicates the relative flow direction).**

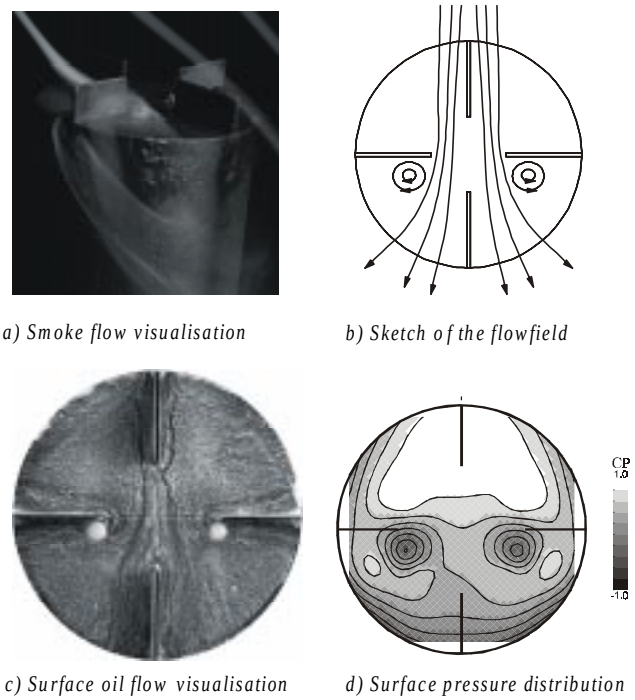


**Fig. 11 Flow over Probe 2b at 30° pitch angle (roll angle: 0°). Two vortices can be seen to form behind the side fences.**

The first potential geometry is that given by probes 2b and 2c, shown in Fig. 2, which are effectively the same as probes 1b and 1c but with a central area free from fences. This leads to a gap in the fence structure that was found to have a significant effect on the flowfield. While a separation bubble is formed downstream of the fences in a similar fashion to probes 1a-c, there is also clear evidence of a vortex immediately behind the edges of the 'gap' in the fence. This is clearly shown in Fig. 11 which compares surface pressure, oil-flow visualisation and smoke flow visualisation for probe 2b at $\theta$=30°, $\phi$=0°. The presence of the vortex causes an additional low pressure field on the downstream half of the probe surface. The strength of this vortex increases with angle of attack,

but decreases with roll angle (up to 45°) as can be seen in the pressure distributions shown in Fig. 12. By comparison with the pressure distributions achieved with the other probes designs it was felt that the presence of such a vortex might be disadvantageous in a 5-sensor probe.

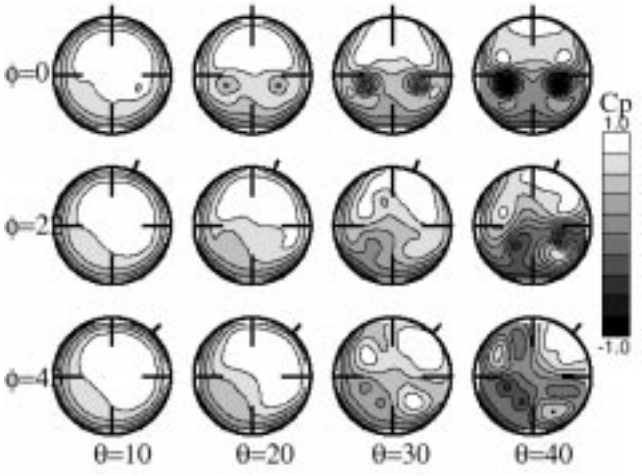


**Fig. 12 Selection of measured surface pressure distributions on Probe 2b for various pitch and roll angles (the flag near the top of each plot indicates the relative flow direction).**

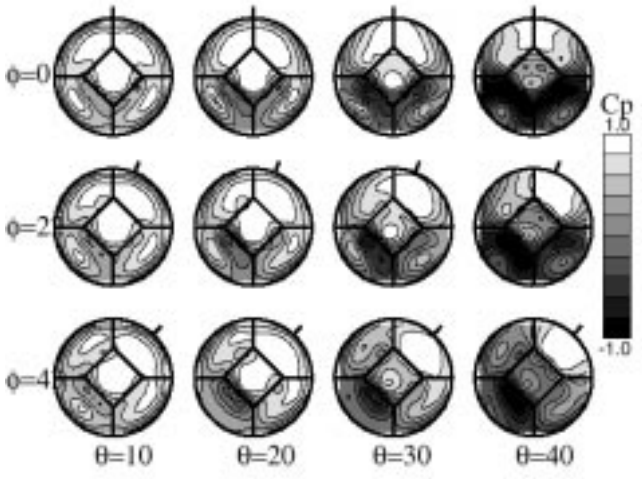


**Fig. 13 Selection of measured surface pressure distributions on Probe 3b for various pitch and roll angles (the flag near the top of each plot indicates the relative flow direction).**

Therefore, a further variation of the design was tested, featuring a central box-section to act as a rudimentary Pitot device while at the same time preventing vortex formation behind the edges of the fences. Selected pressure distributions for one such probe (3b in Fig. 1) are shown in Fig. 13. There is no evidence of any vortices, and the pressure in the central portion of the probe is close to the stagnation pressures for angles of attack up to more than 20°. On the leeward side of the fences similar flow structures to those behind the simple straight fences of probes 1a and 1b can be seen. These results suggest that this probe displays encouraging characteristics for the use as a five-sensor probe.

## EVALUATION OF SUITABILITY FOR 5-HOLE-TYPE PROBES

In order to evaluate the suitability of each design for a 5-sensor probe, the pressures that would be detected by the proposed array of pressure sensors embedded in the surface were calculated from a weighed average of all pressure measurements lying within the area of each sensor. These regions (0 – IV) are indicated in Fig. 14 by the 4/5 large circles each of which surrounds a number of tapping positions.

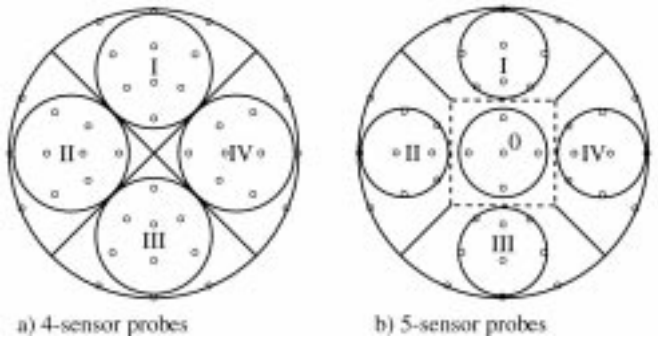


**Fig. 14 Experimental sensor locations for testing.**

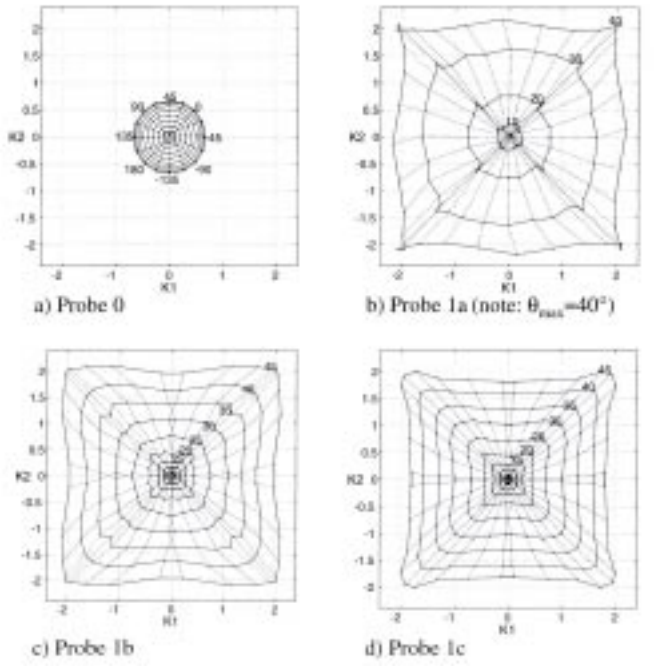


**Fig. 15 Calibration coefficients $K_1$ and $K_2$ for Probes 0 and 1a-c, for pitch angles 0°to 45° in steps of 5° (apart from Probe 1a) and roll angles –180° to +180° in steps of 11.25°.**

The predictions of the pressures that would be measured by an equivalent 5-sensor probe can be used to estimate the calibration characteristics of an equivalent miniature probe. To allow a comparison, the following calibration coefficients were computed:

$$K_1 = \frac{p_I - p_{III}}{q} \quad K_2 = \frac{p_{IV} - p_{II}}{q}$$

$$K_{pt} = \frac{p_t - p_0}{q} \quad K_{dyn} = \frac{p_0 - p_m}{q}$$

where

$$p_m = \frac{p_I + p_{II} + p_{III} + p_{IV}}{4}$$

and $p_t$ is the total pressure (obtained from the Pitot-static tube in the wind tunnel working section). In a typical application the dependency of all four coefficients on flow angle would be determined in a calibration experiment and some iterative procedure can be used to calculate flow velocity and direction from the sensor measurements. It is not suggested here that this is necessarily the most appropriate calibration strategy for a real 5-hole probe, but the above coefficients are useful as a means for comparison of potential geometries and it is the authors' experience that this approach is successful over a wide range of pitch angles. The directional sensitivity of a probe can be assessed from $K_1$ and $K_2$, while the ability to determine the magnitude of flow Mach number (or velocity) throughout a wide range of angles is contained in $K_{pt}$ and $K_{dyn}$. Ideally, $K_1$ and $K_2$ should display a large variation with pitch and roll angle, while $K_{pt}$ and $K_{dyn}$ should be relatively constant for a large range of angles.

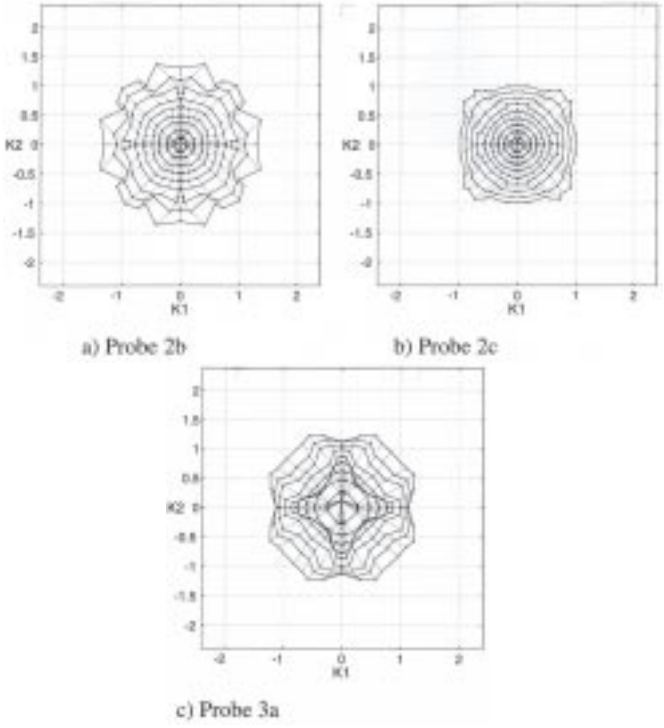


**Fig. 16 Calibration coefficients $K_1$ and $K_2$ for Probes 2b, 2c, 3a.**

There are many different calibration strategies for 5-hole probes and the above is not necessarily the most appropriate in every situation. Several authors[9,10] have shown that more sophisticated techniques can significantly enlarge the range and accuracy of multi-hole probes. For this reason, even designs that appear to be somewhat deficient using the current calibration coefficients may be extended in their operating range if a different calibration strategy were implemented.

Although probes 1a, 1b and 1c do not have a central sensor and can therefore not be used to construct a 5-hole probe, the coefficients $K_1$ and $K_2$ were also calculated for these designs using the corresponding surface pressures. This allows an evaluation of the influence of fences, when compared to an equivalent plot for the strictly planar probe 0. The resulting plots are shown in Fig. 15 giving the range of calibration parameters for pitch angles up to 45° and roll angles between -180° and +180°. It can clearly be seen that the strictly planar probes (Fig. 15a) already displays some directional sensitivity, although its sensitivity in the current calibration system decreases rapidly at pitch angles above 35°. However, the directional sensitivity of a probe is greatly increased by the introduction of fences when in all cases the coefficients increase by approximately a factor of 3.

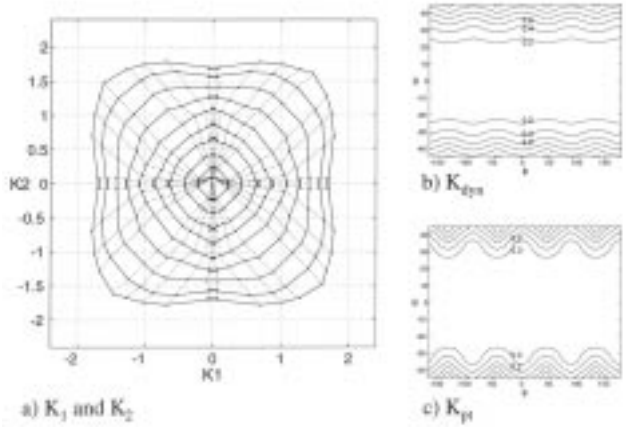


**Fig. 17 Calibration coefficients for Probe 3b for pitch angles 0°to 45° in steps of 5° and roll angles –180° to +180° in steps of 11.25°.**

Fig. 16 shows similar calibration plots obtained for a 5-sensor version of probes 2b, 2c and 3a. It can be seen that neither design exhibits characteristics as good as those seen in Fig. 15 with significant variations in sensitivity throughout the angular range. This is thought to be due to the vortices formed behind openings in the fence structures for probes 2b and 2c and to the absence of fences in the case of probe 3a. Figure 17 shows the distributions of all calibration coefficients for probe 3b and it is clear that the results are very promising. The directional sensitivity is comparable to that obtained by probes 1a-c, while the coefficients $K_{pt}$ and $K_{dyn}$. are relatively constant for a large range of flow angles. It is thought that a probe based on such a design should compare well to traditional 5-hole probes.

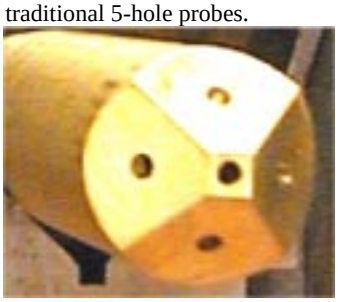

**Fig. 18 Conventional 90° pyramid 5-hole probe**

Fig. 18 shows a conventional truncated 90° pyramid probe. The calibration coefficients for the probe seen in Fig. 18 are given in Fig. 19. It can be seen that the sensitivity of the new probe design of Fig. 17 is comparable and even exceeds that of the traditional probe design (Fig. 19). While this comparison is not exhaustive, it does indicate that the planar probes shapes introduced here have the potential to be at least as sensitive as traditional probe designs, despite their unusual shape.

Within the tested range of Reynolds numbers (between 15,000 and 40,000) the variation of calibration coefficients was inside the

experimental errors. Future work will concentrate on extending the Reynolds number range and the construction of a first MEMS prototype.

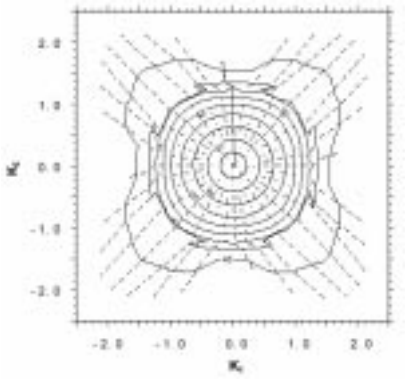

**Fig. 19 Calibration coefficients $K_1$ and $K_2$ for conventional 5-hole probe of Fig. 18 for pitch angles 0°to 45° in steps of 5° and roll angles –180° to +180° in steps of 11.25°.**

## CONCLUSIONS

A novel family of geometries for 5-hole probes, based on a planar array of pressure sensors has been introduced. These shapes have the advantage over traditional designs that they are capable of being manufactured using MEMS technology and therefore offer the potential to build a future fast response sub-miniature flow velocity sensor.

It was shown that even a completely flat cylindrical probe exhibits directional sensitivities that would make it suitable for the design of a 5-sensor probe.

The addition of passive fences fitted to the frontal surface of a cylindrical probe has been shown to significantly increase the sensitivity and usefulness for a potential 5-sensor probe. This was shown to be achieved by the local changes of the flowfield, in particular by the appearance of separation bubbles on the leeward side of the fences.

A geometry suitable for the construction of a 5-sensor probe was identified. The directional sensitivity of such a probe was found to be at least equivalent of that displayed by traditional designs.

## REFERENCES

1 Bryer, D.W. and Pankhurst, R.C., “Pressure-probe methods for determining wind speed and flow direction”, NPL monograph (TJ29), HMSO, 1971

2 Naughton, J.W., Cattafesta, L.N., and Settles, G.S., “Miniature, fast-response five-hole conical probe for supersonic flowfield measurements”, AIAA Journal, Vol.31, No.3, pp. 453-458, March, 1993

3 Ligrani, P.M., Singer, B.A. and Braun, L.R., “Miniature five-hole pressure probe for measurement of three mean velocity components in low-speed flows”, J. Phys. E: Sci. Instrum., Vol.22, pp. 868-876, 1989

4 Mrathe, B.V., Lakshminarayana, B., and Maddock, D.G., “Experimental investigation of steady and unsteady flow field downstream of an automotive torque converter and inside the stator: Part I – flow at exit of turbine”, J. Turbomachinery, Trans. ASME, Vol.119, July 1997, pp. 624-627

5 Madou, M.J. , "Fundamentals of microfabrication", CRC Press, Boca Raton (1997) ISBN 0849394511

6 Elwenspoek, M., Jansen, H., "Silicon Micromachining", Cambridge University Press, Cambridge (1999) ISBN 052159054X

7 Löfdahl, L., Gad-el-Hak, M., “MEMS applications in turbulence and flow control”, Prog. Aero. Sc., Vol.35, pp. 101-203, 1999

8 Rediniotis, O.K., Johansen, E.S, Tsao, T., Seifert, A. and Pack, L.G., "MEMS-based probes for velocity and pressure measurements in unsteady and turbulent flowfields", AIAA paper 99-521, January 1999

9 Redionitis, O.K. and Vijayagopal, R., “Miniature multihole pressure probes and their neural-network-based calibration”, AIAA J., Vol. 37, No. 6, pp. 666-674, 1999

10 Dambach, R, and Hodson, HP, " Tip leakage flow in a radial inflow turbine with varying gap height", 14th International Symposium on Air Breathing Engines, Florence, Italy, Sept. 5-10, 1999